Kinetics and Mechanisms of Anation and Exchange Reactions in Pentakis(*N,N*-dimethylformamide)dioxouranium(VI) Ion in Nonaqueous Media

Hideo Doine, Yasuhisa Ikeda, Hiroshi Tomiyasu, and Hiroshi Fukutomi*

Research Laboratory for Nuclear Reactors, Tokyo Institute of Technology, O-okayama, Meguro-ku, Tokyo 152

(Received December 8, 1982)

The exchange reaction of *N,N*-dimethylformamide (dmf) in $[UO_2(dmf)_5]^{2+}$ ion and the anation reactions by SCN^- and N_3^- have been studied by the NMR method in CD_2Cl_2 and the stopped-flow method in DMF, respectively. For the dmf exchange reaction, rate $=(k_d+k_IK_{os}[DMF])[UO_2(dmf)_5^{2+}]/(1+K_{os}[DMF])$, where k_d, k_I, and K_{os} are $(1.30\pm0.21)\times10^2\ s^{-1}$, $(2.94\pm0.07)\times10^3\ s^{-1}$, and $1.59\pm0.11\ mol^{-1}\ kg$ at $-50\ °C$, respectively. For the anation reactions by SCN^- and N_3^-, the pseudo-first-order rate constant (k_{obsd}) is expressed by $k_{obsd}=\{k_{-1}+(k_1+k_{-1})K_{os}[X]\}/(1+K_{os}[X])$ (X=SCN^- and $[UO_2(dmf)_5]^{2+}$ for the anation reactions by SCN^- and N_3^-, respectively). The values of k_1, k_{-1}, and K_{os} at 25 °C are $1.95\times10^2\ s^{-1}$, $4.27\times10^2\ s^{-1}$, $1.48\times10^2\ M^{-1}$ (1 M=1 mol dm^{-3}), and $1.64\times10^3\ s^{-1}$, $3.72\times10^2\ s^{-1}$, $1.80\times10^2\ M^{-1}$ for SCN^- and N_3^- anation reactions, respectively. These results suggest that the substitution reaction in $[UO_2(dmf)_5]^{2+}$ ion proceeds through the associative interchange mechanism. The difference of reactivities for SCN^- and N_3^- toward $[UO_2(dmf)_5]^{2+}$ ion seems to be related to the pK_a values for acids, HSCN and HN_3.

Ligand exchange reactions in the equatorial plane of uranyl complexes have been extensively studied by using NMR,[1–7] and it is proposed that the ligand exchange reactions in most of the uranyl complexes proceed through the dissociative(D) or dissociative interchange(I_d) mechanism.[8] There have been a few studies on the anation reactions of uranyl aqua complex with some anions in aqueous solution,[9–11] and very few studies have been concerned with the ligand substitution of uranyl complexes in nonaqueous solvent.

Hence a detailed kinetic analysis of ligand substitution reactions for $[UO_2(dmf)_5]^{2+}$ ion was performed for the following reactions,

$$[UO_2(dmf)_5]^{2+} + DMF^* \rightleftharpoons [UO_2(dmf)_4dmf^*]^{2+} + DMF, \quad (1)$$

$$[UO_2(dmf)_5]^{2+} + SCN^- \rightleftharpoons [UO_2(dmf)_4NCS]^+ + DMF, \quad (2)$$

$$[UO_2(dmf)_5]^{2+} + N_3^- \rightleftharpoons [UO_2(dmf)_4N_3]^+ + DMF, \quad (3)$$

where an asterisk is used to denote the exchanging species. The dmf exchange reaction has been already reported by Lincoln *et al.*[5] They studied the dmf exchange by measuring the NMR line-broadening of the methyl protons of free and coordinated DMF and proposed that the dmf exchange proceeded through the D mechanism.

In the present study, the NMR line broadening of the formyl proton in DMF was measured by changing the free DMF concentration over a 50 fold concentration range and compared with the Lincoln's results. The reaction mechanism is discussed by comparing the results of kinetic studies of reactions (1), (2), and (3).

Experimental

Synthesis of Complexes. The $[UO_2(dmf)_5](ClO_4)_2$ complex was prepared in the atomosphere of nitrogen by refluxing hydrated uranyl perchlorate with triethyl orthoformate at 50—60 °C for one hour, followed by the addition of *N,N*-dimethylformamide at room temperature. The resulting light yellow crystals were filtered, washed with ethyl ether and dried *in vacuo* for 2 d. Anal. Calcd for $[UO_2(dmf)_5](ClO_4)_2$: C, 21.59; H, 4.22; N, 8.39. Found: C, 21.65; H, 4.20; N, 8.50. Elemental analysis of the complexes was carried out in the Institute of Physical and Chemical Research.

Other Materials. Dichloromethane-d_2 (CD_2Cl_2, Merck 99%), which was used as a solvent in the exchange reaction of dmf in $[UO_2(dmf)_5]^{2+}$ complex, was died over 4A molecular sieves (Wako Pure Chemical Ind., Ltd.). *N,N*-Dimethylformamide (Wako) was distilled twice under reduced pressure and stored over 4A molecular sieves. Triethyl orthoformate (Wako) was of guaranteed grade and used without further purification. Sodium thiocyanate (Wako) was used without further purification. The concentration of azide ion in DMF solution was determined by measuring sodium ion concentration with a Varian-Techtron 1100 flamespectrophotometer. The amount of water contained in DMF solvent was measured by a Mitsubishi CA-02 moisturemeter and the maximum concentration was found to be less than 0.01 M. Anhydrous sodium prechlorare (Wako) was used to adjust the ionic strength of solutions.

Preparations of NMR Samples. Sample solutions for NMR measurements were prepared by weighing sample substances in a 1 cm^3 volumetric flask and some of each solution was placed in an NMR sample tubes and sealed. All samples were prepared in a glove box filled with dry nitrogen. Sample solutions were placed in a dark room to avoid the photochemical redox reactions.[12]

Measurement of NMR and IR Spectra. ^1H NMR spectra were measured at 100 MHz on a JEOL JNM-FX 100 FT-NMR spectrometer equipped with a JNM-VT-3B temperature controller. Infrared spectra of $[UO_2(dmf)_5]^{2+}$ complex in CD_2Cl_2 were recorded in 200—4000 cm^{-1} range by using a JASCO DS-701G IR spectrophotometer.

Measurement of Equilibrium Constants. The equilibrium constants between $[UO_2(dmf)_5]^{2+}$ and SCN^- or N_3^- ions were measured spectrophotometrically by using a Shimadzu UV-210A double-beam spectrophotometer with a cell compartment thermostated at 25 °C. The ionic strength of sample solutions was adjusted to 0.2 M by using sodium perchlorate.

Kinetic Measurements. The dmf exchange reaction in $[UO_2(dmf)_5]^{2+}$ complex was measured by the NMR line-broadening method as described in the previous paper.[13]

As is mentioned later, the methyl proton signal of the coordinated dmf, which should have two peaks, gave a single peak. This implies that the use of the methyl proton signal for the kinetic measurements is liable to produce an uncertain error. From this reason, the formyl proton signal was employed in the present study.

The anation rates were measured by using a Durrum 110 stopped-flow spectrophotometer with a thermostated cell compartment. The pseudo-first-order rate constants were obtained from the plot of $\ln\{(A_t-A_\infty)/(A_0-A_\infty)\}$ *vs.* time. The symbols, A_0, A_∞, and A_t represent the absorbance at time zero, infinity, and t, respectively.

Results and Discussion

Structure of $[UO_2(dmf)_5](ClO_4)_2$ *in* CD_2Cl_2. Figure 1 shows the ^1H NMR spectrum of a solution containing $[UO_2(dmf)_5](ClO_4)_2$, DMF, and CD_2Cl_2 at -80 °C. From the comparison with the ^1H NMR spectrum of pure DMF, the signals (a) and (b) were assigned to the methyl protons of free and coordinated DMF, respectively. The signals (c) and (d) were attributed to the formyl protons of free and coordinated DMF, respectively. It is noted that the methyl proton signal of the coordinated dmf is a single peak, while that of the free DMF has two equivalent peaks. This result is consistent with that of Lincoln *et al.*[5] The signal of methyl protons of the coordinated dmf should originally have two peaks. In fact, this kind of single peak has not been observed in other dmf complexes, *e.g.* $[Al(dmf)_6]^{3+}$, $[Ga(dmf)_6]^{3+}$, and $[Be(dmf)_4]^{2+}$.[14-16] This phenomenon may be due to the rotation round the C–N bond in coordinated dmf molecules, which is assumed to be too fast on the NMR time scale at this temperature, or to the equalization of chemical shifts of both methyl groups of the coordinated dmf molecules caused by the magnetic anisotropy of the uranyl ions as proposed by Lincoln *et al.*[5] The former is not likely because the IR spectrum of $[UO_2(dmf)_5]^{2+}$ complex in CD_2Cl_2 gives the value of 1642 cm^{-1} for the C–O stretching of dmf, which is 33 cm^{-1} lower than that observed for pure DMF (1675 cm^{-1}). This fact suggests that the dmf molecules coordinate to the uranyl ion through oxygen, since the C–O stretching, so called Amide I, is shifted to a lower side when the dmf molecule coordinates to metal ion through oxygen.[17-19] This coordination tends to increase the double bond character of the C–N group and hence make more difficult the rotation round the C–N bond.

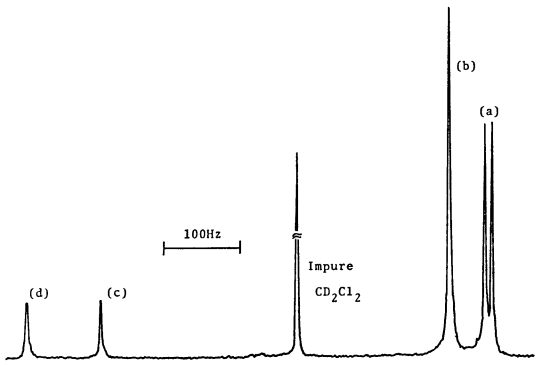

Fig. 1. The ^1H NMR spectrum of a solution consisting of $[UO_2(dmf)_5]^{2+}$ (0.00433 mol kg^{-1}), DMF (0.0216 mol kg^{-1}), and CD_2Cl_2 (11.4 mol kg^{-1}) at -80 °C.

On the other hand, it is more likely that the magnetic anisotropy of the uranyl ion may introduce the degeneration of two signal peaks arising from the methyl groups of the coordinated dmf. Pople *et al.*[20] give the equation for the chemical shift ($\Delta\delta$) caused by the anisotropic field

$$\Delta\delta = \Delta\chi_{atomic}(1-3\cos^2\gamma)/3R^3, \quad (4)$$

where $\Delta\chi_{atomic} = \chi_{atomic}$(parallel to axis) $- \chi_{atomic}$ (perpendicular to axis), in which the axis is taken to be the O=U=O axis, R is the distance between the proton and the uranium atom, and γ is the angle between a straight line connecting the proton and uranium atom and the O=U=O axis. From this equation, it is expected that the chemical shifts of both methyl groups of the coordinated dmf become identical at the particular values of γ and R. Lincoln *et al.*[5] estimated the value of $\Delta\delta$ for both methyl groups of the coordinated dmf by using Eq. 4 and found that the calculated values were consistent with the experimental ones. Furthermore, the dmf methyl proton signal of $UO_2(acac)_2dmf$ (acac=acetylacetonate) in CD_3COCD_3 and CD_2Cl_2 has two equivalent peaks[12] in spite of the coordination of dmf in the same equatorial plane of uranyl ion and the differences of chemical shifts between two peaks are 0.03 and 0.14 ppm in CD_3COCD_3 and CD_2Cl_2, respectively. These phenomena can be explained by the differences of the values for γ and R in $UO_2(acac)_2dmf$ and $[UO_2(dmf)_5]^{2+}$ complexes.

The number of the coordinated dmf molecules were determined by area integrations of the methyl and formyl proton signals of free and coordinated DMF, respectively and the results are listed in Table 1. The absence of any significant variation of the number

Table 1. Solution compositions and coordination numbers (CN) for the exchange of dmf in $[UO_2(dmf)_5]^{2+}$

No.	$[UO_2(dmf)_5^{2+}]$ / 10^{-3} mol kg^{-1}	DMF / 10^{-2} mol kg^{-1}	$[CD_2Cl_2]$ / mol kg^{-1}	CN[a]
i	2.54	0.871	11.5	5.2±0.1
ii	4.33	2.16	11.4	5.1±0.3
iii	4.59	5.24	11.4	5.1±0.1
iv	4.30	9.73	11.4	4.8±0.2
v	21.7	44.0	10.9	5.0±0.1

a) The quoted errors represent the standard deviations.

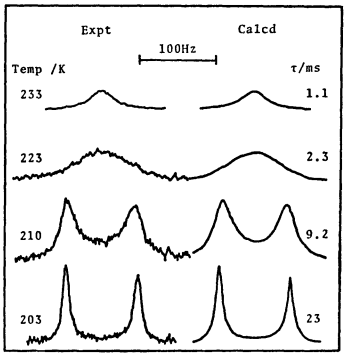

Fig. 2. Experimental (left-hand side) and best-fit calculated ^1H NMR lineshapes of a solution consisting of $[UO_2(dmf)_5]^{2+}$ (0.00433 mol kg^{-1}), DMF (0.0216 mol kg^{-1}), and CD_2Cl_2 (11.4 mol kg^{-1}). Temperatures and best-fit τ-values are shown at left- and right-hand side of the figure, respectively.

of coordinated dmf molecules over a wide concentration range (Table 1) indicates that neither CD_2Cl_2 nor perchlorate ion enters into the first coordination sphere of uranyl ion. The absence of any splitting of the coordinated dmf formyl proton signal indicates also that the five molecules of the coordinated dmf occupy the equivalent equatorial positions of the uranyl ion. These results confirm that the structure of $[UO_2(dmf)_5]^{2+}$ ion in CD_2Cl_2 is pentagonal bipyramidal.

Exchange Reaction of DMF in $[UO_2(dmf)_5]^{2+}$ Ion in CD_2Cl_2. A typical temperature dependence of lineshape for the formyl proton signals of the coordinated and free DMF is shown at the left side in Fig. 2. This figure shows that the dmf exchange reaction occurs between the coordinated and free sites. The best-fit life times (τ-values) were determined by using the computer program for two site exchange[21] and are shown at the right side in Fig. 2 together with the corresponding lineshapes. From these τ-values, the first-order rate constants, k_{ex}, were calculated by the following equations,

$$\tau = P_F\tau_c = P_c\tau_F, \tag{5}$$

$$k_{ex} = 1/\tau_c = \text{rate}/5[UO_2(dmf)_5^{2+}] = (kT/h)\exp(-\Delta H^*/RT)\exp(\Delta S^*/R), \tag{6}$$

where τ and P with the subscripts of F and c are the life times and mole fractions of the free and coordinated sites, respectively.

The same measurements were carried out for the solutions with different compositions listed in Table 1. Figure 3 shows the plots of k_{ex} against the DMF concentration, which do not yield a simple linear relationship but the intercepts and the limiting values at high concentration region. This result suggests that the dmf exchange reaction proceeds through two paths, that is, one is the independent path of the DMF concentration and another is the path which depends on the DMF concentration in its low region and becomes independent of the DMF concentration in its high region.

These paths are assumed to proceed through the D and I mechanism[8] as follows.

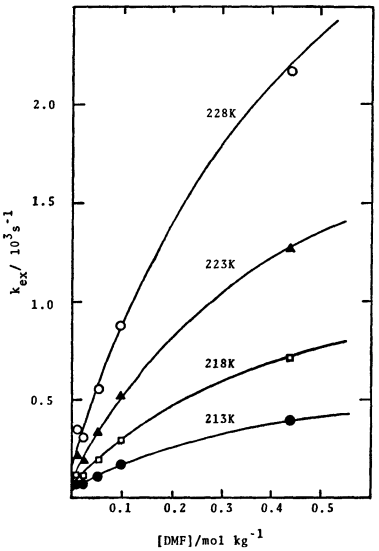

Fig. 3. Plots of k_{ex} *vs.* [DMF] for the exchange of dmf in $[UO_2(dmf)_5]^{2+}$. The solid lines denote the least-squares best-fit lines.

$$[UO_2(dmf)_5]^{2+} + DMF^* \xrightarrow[\text{slow}]{k_d} [UO_2(dmf)_4]^{2+} + DMF + DMF^* \xrightarrow[\text{fast}]{} [UO_2(dmf)_4dmf^*]^{2+} + DMF,$$

$$[UO_2(dmf)_5]^{2+} + DMF^* \overset{K_{os}}{\rightleftharpoons} [UO_2(dmf)_5]^{2+}\cdots DMF^* \xrightarrow[\text{slow}]{k_I} [UO_2(dmf)_4dmf^*]^{2+}\cdots DMF \xrightarrow[\text{fast}]{} [UO_2(dmf)_4dmf^*]^{2+} + DMF,$$

where K_{os} is the outer-sphere complex formation constant. These mechanisms lead to the following equation for k_{ex}[22]

$$k_{ex} = \frac{k_d + k_I K_{os}[DMF]}{1 + K_{os}[DMF]}. \tag{7}$$

This equation can be simplified to $k_{ex} = k_d + k_I K_{os} \times [DMF]$ when $K_{os}[DMF] \ll 1$. This corresponds to the dependence of k_{ex} on the DMF concentration in the low concentration region. If the value of $K_{os}[DMF]$ is much larger than unity, Eq. 7 becomes $k_{ex} \simeq k_I$, which agrees with the fact that the dmf exchange rate becomes independent of the DMF concentration in its high region.

The values of k_d, k_I, and K_{os} were calculated by

Table 2. Kinetic parameters of ligand exchange reaction[a]

Temp / K	k_d / 10^2 s^{-1}	k_I / 10^3 s^{-1}	K_{os} / mol^{-1} kg
228	2.10±0.39	5.08±0.12	1.59±0.19
223	1.30±0.21	2.94±0.07	1.59±0.11
218	0.72±0.10	1.51±0.03	1.88±0.06
213	0.43±0.05	0.83±0.01	1.88±0.03

a) The quoted errors represent the standard deviations.

Table 3. Kinetic data for the ligand substitution reactions in $[UO_2(dmf)_5]^{2+}$ at 298 K

Ligand	Solvent	Method	Rate constant / s^{-1}	Mechanism	ΔH^{*} b) / kJ mol^{-1}	ΔS^{*} b) / J K^{-1} mol^{-1}
DMF	CD_2Cl	NMR	$k_d=4.70\times10^4$	D	42.0±2.1	−15.1±3.3
			$k_I=2.34\times10^6$	I	48.3±0.9	38.6±2.6
SCN^-	DMF	Stopped-flow	$k_1=1.95\times10^{2}$ a)	I	67.6±3.5	24.4±4.0
			$k_{-1}=4.27\times10^{2}$ a)	—	38.6±3.1	−68.0±5.7
N_3^-	DMF	Stopped-flow	$k_1=1.64\times10^{3}$ a)	I	50.6±2.0	−14.5±4.8
			$k_{-1}=3.72\times10^{2}$ a)	—	47.2±2.3	−38.0±7.2

a) Ionic strength=0.2 M($NaClO_4$). b) The quoted errors represent the standard deviations.

using the nonlinear least-squares method. The results are shown in Table 2. The solid lines in Fig. 3 are the best-fit lines obtained from the calculated values of k_d, k_I, and K_{os} and indicate that the calculated values are in fair agreement with the experimental data. The activation parameters for k_d and k_I were obtained from the Eyring plot and are listed in Table 3.

The present results are different from those of Lincoln *et al.*[5] They reported that the rate of dmf exchange was independent of the free DMF concentration and that this exchange reaction proceeded through the D mechanism. In their experiments, the first-order rate constants are obtained from the lineshape analysis of the methyl proton signals of the free and coordinated DMF and the concentration range of free DMF (0.00213—0.04323 M) is lower than that of the present experiment (0.0123—0.588 M). Hence the different results in two works might be due to the differences in the experimental conditions.

Equilibrium between $[UO_2(dmf)_5]^{2+}$ and SCN^-. Figure 4 shows spectral changes of $[UO_2(dmf)_5]^{2+}$ with varying the concentration of thiocyanate ion from 0.01 M to 0.04 M in DMF. Although an isosbestic point is not observed, the most probable reaction corresponding to the spectral change is

$$[UO_2(dmf)_5]^{2+} + SCN^- \underset{}{\overset{K}{\rightleftharpoons}} [UO_2(dmf)_4NCS]^+ + DMF. \quad (8)$$

The equilibrium constant K for this process was obtained from the following equation.

$$\frac{[UO_2(dmf)_5^{2+}]}{Abs-\varepsilon_1[UO_2(dmf)_5^{2+}]} = \frac{1}{\varepsilon_2-\varepsilon_1} + \frac{1}{(\varepsilon_2-\varepsilon_1)K[SCN^-]}, \quad (9)$$

where Abs is the observed absorbance, and ε_1 and ε_2 are the molar extinction coefficients of $[UO_2(dmf)_5]^{2+}$ and $[UO_2(dmf)_4NCS]^+$, respectively. If $[UO_2(dmf)_5^{2+}]/(Abs-\varepsilon_1[UO_2(dmf)_5^{2+}])$ is plotted against $1/[SCN^-]$, the plot should be linear. Indeed, Fig. 5 shows this linear relationship, which supports the validity of the reaction given by Eq. 8. From the slope and the intercept, the value of K was calculated and is listed in Table 4.

Equilibrium between $[UO_2(dmf)_5]^{2+}$ and N_3^-. When azide ions were added to a DMF solution of $[UO_2(dmf)_5]^{2+}$, a change in the absorption spectrum of $[UO_2(dmf)_5]^{2+}$ was much larger than that by the addition of thiocyanate ion. Therefore, the measurement of the equilibrium constant K for $[UO_2(dmf)_4N_3]^+$, was carried out under the conditions of $[UO_2(dmf)_5^{2+}] \gg [N_3^-]$ in order to avoid other complex formation. In this case, the value of K was calculated from the slope and the intercept in the plot of $[N_3^-]/(Abs-\varepsilon_1[UO_2(dmf)_5^{2+}])$ *vs.* $1/[UO_2(dmf)_5^{2+}]$ at 437 nm. The result is shown in Table 4.

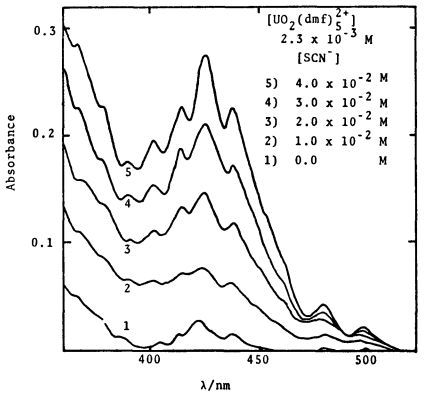

Fig. 4. The spectral change of $[UO_2(dmf)_5]^{2+}$ with varying the concentration of thiocyanate ion in DMF at 25 °C and μ=0.2 M ($NaClO_4$).

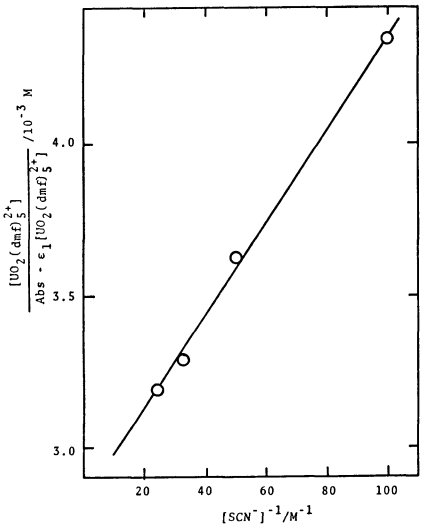

Fig. 5. The plot of $[UO_2(dmf)_5^{2+}]/(Abs-\varepsilon_1[UO_2(dmf)_5^{2+}])$ *vs.* $[SCN^-]^{-1}$ for the substitution reaction of $[UO_2(dmf)_5]^{2+}$ by thiocyanate ion at 25 °C, 437 nm, and μ=0.2 M ($NaClO_4$).

Anation Reaction. On the basis of the results of equilibrium constants measured spectrophotometrically, the pseudo-first-order rate constants, k_{obsd}, for the anation reactions by SCN^- and N_3^- were measured under the conditions of $[SCN^-]>[UO_2(dmf)_5^{2+}]$ and $[UO_2(dmf)_5^{2+}]>[N_3^-]$, respectively.

Figures 6 and 7 show the plots of k_{obsd} against $[SCN^-]$ and $[UO_2(dmf)_5^{2+}]$, respectively, which do not display a simple linear relationship, and the values of k_{obsd} approach each limiting value at high concentration region of $[SCN^-]$ and $[UO_2(dmf)_5^{2+}]$. Attempts were also made to examine the effect of the water on the anation reaction, in which the concentration of water was changed from 0.01 M to 0.1 M. It was found that water made no effect on the present anation reaction in this concentration range.

Table 4. Equilibrium constants at 298 K[a)]

Ligand	K / M^{-1}	K_{calcd} / M^{-1}
SCN^-	186±26	215±42
N_3^-	974±73	974±43

Ionic strength=0.2 M($NaClO_4$). a) The quoted errors represent the standard deviations.

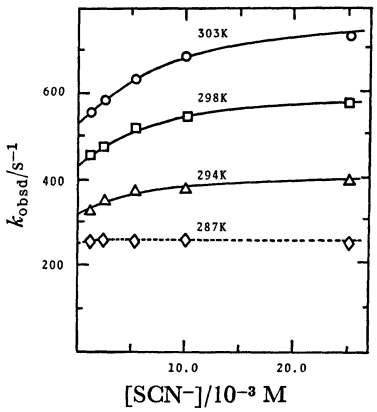

Fig. 6. Plots of k_{obsd} *vs.* $[SCN^-]$ for the anation reaction by SCN^-.
The solid lines denote the least-squares best-fit lines.

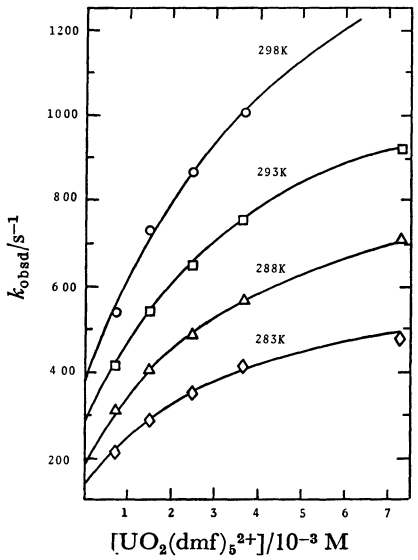

Fig. 7. Plots of k_{obsd} *vs.* $[UO_2(dmf)_5^{2+}]$ for the anation reaction by N_3^-.
The solid lines denote the least-squares best-fit lines.

Taking into account the result that the dmf exchange reaction in $[UO_2(dmf)_5]^{2+}$ seems to proceed predominantly through the I mechanism as described above, the following I mechanism appears to be the most plausible mechanism for the present anation reactions.

$$[UO_2(dmf)_5]^{2+} + L^- \overset{K_{os}}{\rightleftharpoons} [UO_2(dmf)_5]^{2+}\cdots L^-$$

$$[UO_2(dmf)_5]^{2+}\cdots L^- \underset{k_{-1}}{\overset{k_1}{\rightleftharpoons}} [UO_2(dmf)_4L]^+ + DMF,$$

where L^- is the SCN^- or N_3^- ion, and K_{os} is the outer-sphere complex formation constant. According to this mechanism, the observed rate constant, k_{obsd}, is given by Eq. 10

$$k_{obsd} = \frac{k_{-1}+(k_1+k_{-1})K_{os}[X]}{1+K_{os}[X]} \quad (10)$$

where X is SCN^- and $[UO_2(dmf)_5]^{2+}$ for the anation reactions by SCN^- and N_3^-, respectively, since these anation reactions were carried out under the conditions of $[UO_2(dmf)_5^{2+}]<[SCN^-]$ and $[UO_2(dmf)_5^{2+}]>[N_3^-]$, respectively. When $K_{os}[X]\ll 1$, Eq. 10 can be simplified to $k_{obsd}=k_{-1}+(k_1+k_{-1})K_{os}[X]$. This is in good agreement with the dependence of k_{obsd} on [X] in the low concentration region. If the value of $K_{os}[X]$ is much larger than unity, Eq. 10 becomes $k_{obsd}=k_1+k_{-1}$, which is consistent with the fact that the limiting values of k_{obsd} are obtained at high [X].

The values of k_1, k_{-1}, and K_{os} were calculated by the nonlinear least-squares method and are listed in Table 5. The solid lines obtained from the calculated values agree with the experimental results. The activation parameters for k_1 and k_{-1} obtained from the Eyring plots are shown in Table 3.

The outer-sphere complex formation constants for both reactions are nearly the same as shown in Table 5, while the interchange rate constants are fairly different. This seems to be reasonable since SCN^- and N_3^- ions have the same charge, nearly the same size and structure. Thus the interatomic distance between $[UO_2(dmf)_5]^{2+}$ and SCN^- or N_3^- in the outer-sphere

Table 5. Kinetic parameters of ligand substitution reaction[a)]

Temp / K	k_1 / s^{-1}	k_{-1} / s^{-1}	K_{os} / M^{-1}
$[UO_2(dmf)_5]^{2+}+SCN^-$			
293	116±8	320±25	154
298	195±12	427±30	148
303	273±19	528±35	126
$[UO_2(dmf)_5]^{2+}+N_3^-$			
283	520±35	132±12	300
288	784±37	181±15	270
293	1077±41	274±21	220
298	1640±49	372±30	180

Ionic strength=0.2 M($NaClO_4$). a) The quoted errors represent the standard deviations.

complexes is assumed to be the same. In this case, the Fuoss equation[23] gives the same value for the outer-sphere complex formation constant. When the anation reaction proceeds through the interchange mechanism, the relationship between the equilibrium constant (K) and the outer-sphere complex formation constant (K_{os}) is generally given by the following equation.[24]

$$K = K_{ob}(1+k_1/k_{-1}) \quad (11)$$

The calculated values of K were obtained from Eq. 11 by using the values of k_1, k_{-1}, and K_{os} derived from kinetic measurements. It is found that the calculated K values (Table 4) are in remarkable agreement with those obtained spectrophotometrically. This fact also supports that the anation reactions by SCN^- and N_3^- proceed through the interchange mechanism. Table 3 indicates that the interchange rate constants (k_1) for the anation by SCN^- and N_3^- are smaller than that of dmf exchange reaction by a factor of about 10^3, and the values of ΔH^* for the anation reactions are larger than that for the dmf exchange reaction. These facts suggest that the anation reactions by SCN^- and N_3^- proceed through the associative interchange (I_a) mechanism. If the anation reaction proceeds through the dissociative interchange (I_d) mechanism, the interchange rate constants and ΔH^* values for the anation reactions should be consistent with those for the dmf exchange reaction. Additional evidence for the I_a mechanism is given by the interchange rate constants k_1 (Table 5), which depend strongly on the nature of the entering ligands SCN^- and N_3^-. The difference of the reactivities, *i.e.* $k_1^{N_3^-}/k_1^{SCN^-} \approx 10$, cannot be attributed to the outer-sphere complex formation, because the value of this ratio is much larger than the corresponding value for K_{os}, $K_{os}^{N_3^-}/K_{os}^{SCN^-}=1.2$ at 25 °C. Thus the different reactivity may be due to a difference in the nucleophilicity of SCN^- and N_3^- toward $[UO_2(dmf)_5]^{2+}$. The value of pK_a for HN_3 is much larger than that for HSCN.

It is concluded that the anation reactions by SCN^- and N_3^- proceed through the I_a mechanism since the interchange rate constants depend strongly on the nature of entering ligands, SCN^- and N_3^-. If it is reasonable to regard the anation reaction as a special case of the solvent exchange reaction where an anion in the second coordination sphere becomes the entering ligand rather than a solvent molecule in the same region,[22] it may be supposed that the k_I path in the dmf exchange reaction also proceeds through the I_a mechanism.

The authors wish to express their thanks to Dr. Roderick D. Cannon of the University of East Anglia, Messrs. Takashi Kojima and Masayuki Harada for their helpful discussions. This work was partly supported by the Grant-in-Aid for Scientific Research from the Ministry of Education, Science and Culture.

References

1) Y. Ikeda, S. Soya, H. Tomiyasu, and H. Fukutomi, *J. Inorg. Nucl. Chem.*, **41**, 1333 (1979).
2) Y. Ikeda, H. Tomiyasu, and H. Fukutomi, *Bull. Res. Lab. Nucl. Reac.*, **4**, 47 (1979).
3) R. P. Bowen, S. F. Lincoln, and E. H. Williams, *Inorg. Chem.*, **15**, 2126 (1976).
4) J. Crea, R. Digiusto, S. F. Lincoln, and H. E. Williams, *Inorg. Chem.*, **16**, 2825 (1977).
5) R. P. Bowen, G. J. Honan, S. F. Lincoln, T. M. Spotswood, and E. H. Williams, *Inorg. Chim. Acta*, **33**, 235 (1979).
6) G. J. Honan, S. F. Lincoln, and E. H. Williams, *J. Chem. Soc., Dalton Trans.*, **1979**, 1220.
7) A. M. Hounslow, S. F. Lincoln, P. A. Marshall, and E. H. Williams, *Aust. J. Chem.*, **34**, 2543 (1981).
8) C. H. Langford and H. B. Gray, "Ligand Substitution Processes," Benjamin, London (1974).
9) M. P. Whiiaker, E. M. Eyring, and E. Dibble, *J. Phys. Chem.*, **69**, 2319 (1965).
10) P. Hurwitz and K. Kustin, *J. Phys. Chem.*, **71**, 324 (1967).
11) A. Ekstrom and D. A. Johnson, *J. Inorg. Nucl. Chem.*, **36**, 2549 (1974).
12) E. Rabinowitch and R. L. Belford, "Spectroscopy and Photochemistry of Uranyl Compounds", Pergamon Press, New York (1964).
13) Y. Ikeda, H. Tomiyasu, and H. Fukutomi, *Bull. Chem. Soc. Jpn.*, **56**, 1060 (1983).
14) W. G. Movius and N. A. Matwiyoff, *Inorg. Chem.*, **6**, 847 (1967).
15) W. G. Movius and N. A. Matwiyoff, *Inorg. Chem.*, **8**, 925 (1969).
16) N. A. Matwiyoff and W. G. Movius, *J. Am. Chem. Soc.*, **89**, 6077 (1967).
17) W. Gerrard, M. F. Lappert, H. Pyszora, and J. W. Wallis, *J. Chem. Soc.*, **1960**, 2144.
18) C. D. Schmulbach and R. S. Drago, *J. Am. Chem. Soc.*, **82**, 4484 (1960).
19) S. J. Kuhn and J. S. McIntyre, *Can. J. Chem.*, **43**, 375 (1965).
20) J. A. Pople, W. G. Schneider, and H. G. Bernstein, "High Resolution Nuclear Magnetic Resonance," McGraw-Hill, New York, N. Y. (1959).
21) G. Binsch, "Topics in Stereochemistry," ed by E. L. Eliel and N, L. Allinger, Wiley Interscience, New York (1968), Vol. 3, p. 97.
22) S, T. D. Lo and T. W. Swaddle, *Inorg. Chem.*, **15**, 1881 (1976).
23) R. M. Fuoss, *J. Am. Chem. Soc.*, **89** 5059 (1958).
24) S. Yamada and M. Tanaka, *J. Inorg. Nucl. Chem.*, **37**, 587 (1975).